

Squared form factors of valence-shell excitations of atomic argon studied by high-resolution inelastic x-ray scattering

X. Kang,^{1,4} K. Yang,^{2,*} Y. W. Liu,^{1,4} W. Q. Xu,^{1,4} N. Hiraoka,³ K. D. Tsuei,³ P. F. Zhang,⁴ and L. F. Zhu^{1,4,†}

¹*Hefei National Laboratory for Physical Sciences at Microscale, University of Science and Technology of China, Hefei, Anhui 230026, People's Republic of China*

²*Shanghai Institute of Applied Physics, Chinese Academy of Sciences, Shanghai 201204, People's Republic of China*

³*National Synchrotron Radiation Research Center, Hsinchu 30076, Taiwan, Republic of China*

⁴*Department of Modern Physics, University of Science and Technology of China, Hefei, Anhui 230026, People's Republic of China*

(Received 18 July 2012; published 10 August 2012)

State-resolved squared form factors of the electric monopolar excitations to $3p^5 4p[1/2]_0$ and $3p^5 4p'[1/2]_0$, the electric dipolar excitations to $3p^5 4s[3/2]_1$ and $3p^5 4s'[1/2]_1$, and the electric quadrupolar excitations to $3p^5 4p[5/2]_2$, $3p^5 4p[3/2]_2$, and $3p^5 4p'[3/2]_2$ of argon are determined by inelastic x-ray scattering with a high resolution of 70 meV. Good agreement is observed between the present results and the calculations of the random phase approximation with exchange except that the present results of $3p^5 4s'[1/2]_1$ in $q^2 > 3$ a.u. are smaller and $3p^5 4p[1/2]_0$ in $q^2 < 1.5$ a.u. are larger than the theoretical results. The difference may be due to the difficulty of obtaining accurate wave functions or dealing with the electronic correlations for a heavier atom such as argon. The disagreements between the present squared form factors and the ones measured by electron energy loss spectroscopy indicate that the first Born approximation is not satisfied, even at an incident electron energy of 2500 eV.

DOI: [10.1103/PhysRevA.86.022509](https://doi.org/10.1103/PhysRevA.86.022509)

PACS number(s): 32.30.Rj, 32.70.Cs, 34.50.Fa

I. INTRODUCTION

The form factor of an atom or molecule, i.e., the transition matrix element, is of great importance because it varies with the momentum and can reveal the momentum distribution character of the wave functions of the initial and final states [1]. The experimental squared form factors (SFF's) with high accuracy can be used to test the theoretical models and calculational codes rigorously. Traditionally, the squared form factors are determined by high-energy electron energy loss spectroscopy (EELS) on the condition that the first Born approximation (FBA) is satisfied. Recently, with the dramatic progress of the third-generation synchrotron radiation photon source, the experimental technique of the inelastic x-ray scattering (IXS) has been applied to measure the squared form factors of atoms or molecules in gas phase [2–4]. The recent IXS works [3,5] show that for the electron impact method the intramolecular multiple scattering has great influence on the cross sections in the large momentum transfer region, even for several kilo-electron-volt impact energies. Since the FBA is valid in IXS, the SFF's determined by IXS give a cross-check to the ones measured by traditional EELS [6–9] and provide an experimental benchmark to test theoretical methods [10–15] in which the electronic correlations and exchange effect are dealt with differently.

Although nonresonant IXS has been widely used to reveal physical information of condensed matter, experiments that take advantage of IXS to investigate the dynamic behaviors of the discrete excitations of atoms or molecules in gas phase are relatively rare due to the extremely low cross section and target density. These experiments include investigations of the valence-shell excitations of He [2,4], Ne [5], and N₂ [3,16], as

well as those of the inner-shell excitations of N₂, N₂O, and CO₂ [17], to the best of our knowledge. These pioneering works give valuable information on electronic excitations without the influence of proximate atoms in condensed matter.

As for argon, previous experiments measuring the dynamic parameters of its valence-shell excitations were mostly carried out by EELS with low-energy [18–21] (<100 eV), moderate-energy [6,9] (300–500 eV), as well as high-energy [7,8,12,22–25] (600 eV–25 keV) electron impact. Particularly, the state-resolved generalized oscillator strengths (GOS's) or apparent GOS's for the electric monopolar excitations to $3p^5 4p[1/2]_0$ and $3p^5 4p'[1/2]_0$ [8,9], the electric dipolar excitations to $3p^5 4s[3/2]_1$ and $3p^5 4s'[1/2]_1$ [6,8], and the electric quadrupolar excitations to $3p^5 4p[5/2]_2$, $3p^5 4p[3/2]_2$, and $3p^5 4p'[3/2]_2$ [8,9] were determined. In addition, some theoretical calculations, such as the FBA [12,26], the first Born and Glauber approximations [23,27], Hartree-Fock (HF) [10,11], and random phase approximation with exchange (RPAE) [10,11], have investigated the GOS's of the valence-shell excitations of argon. By comparing the theoretical calculations with the experimental IXS results, the magnitude of the contribution made by different interactions can be estimated, and the significance of these interactions in different excitation processes can be evaluated.

The squared form factor $\zeta(\mathbf{q}, \omega_n)$ is defined as [1,4] (atomic units are used throughout this paper)

$$\zeta(\mathbf{q}, \omega_n) = \left| \langle \Psi_n | \sum_{j=1}^N \exp(i\mathbf{q} \cdot \mathbf{r}_j) | \Psi_0 \rangle \right|^2. \quad (1)$$

Here \mathbf{q} is the vector of momentum transfer, while Ψ_n and Ψ_0 stand for the final and initial wave functions of the target, respectively. The sum is over all electrons and \mathbf{r}_j is the position vector of the j th electron. $\zeta(\mathbf{q}, \omega_n)$ can be determined from the experimental differential cross section (DCS) of IXS or the

*yangke@sinap.ac.cn

†lfzhu@ustc.edu.cn

high-energy EELS [4,28,29]:

$$\begin{aligned}\zeta(\mathbf{q}, \omega_n) &= \frac{1}{r_0^2} \frac{\omega_i}{\omega_f} \frac{1}{|\boldsymbol{\varepsilon}_i \cdot \boldsymbol{\varepsilon}_f^*|^2} \left(\frac{d\sigma}{d\Omega} \right)_\gamma, \\ &= \frac{1}{4} \frac{k_i}{k_f} q^4 \left(\frac{d\sigma}{d\Omega} \right)_e, \\ &= \frac{q^2}{2\omega_n} f(\mathbf{q}, \omega_n).\end{aligned}\quad (2)$$

The factor $|\boldsymbol{\varepsilon}_i \cdot \boldsymbol{\varepsilon}_f^*|^2$ comes from the polarized direction of incident and scattered photons, and it equals $\cos^2 2\theta$ (2θ is the scattering angle) for completely linear polarized photons with the polarized direction in the horizontal scattering plane. r_0 is the classic electron radius, while ω_i , ω_f and $\omega_n = \omega_i - \omega_f$ stand for the energies of incident and scattered photons and energy loss, respectively. $(\frac{d\sigma}{d\Omega})_\gamma$ and $(\frac{d\sigma}{d\Omega})_e$ stand for the DCS's measured by IXS and the high-energy EELS, while $f(\mathbf{q}, \omega_n)$ is the GOS. k_i and k_f are the momenta of the incident and scattered electrons.

In the present work, the SFF's for the electric monopolar excitations to $3p^5 4p[1/2]_0$ and $3p^5 4p'[1/2]_0$, the electric dipolar excitations to $3p^5 4s[3/2]_1$ and $3p^5 4s'[1/2]_1$, and the electric quadrupolar excitations to $3p^5 4p[5/2]_2$, $3p^5 4p[3/2]_2$, and $3p^5 4p'[3/2]_2$ of argon were measured. The profiles of $\zeta(\mathbf{q}, \omega_n)$ for these excitations are analyzed and the positions of the extrema are determined.

II. EXPERIMENTAL METHOD

The present IXS measurement of argon was carried out at the Taiwan Beamline BL12XU of SPring-8 at a photon energy of about 10 keV and an energy resolution of about 70 meV. The experimental setups and method used in this work were described in our previous works [2,4] in detail. With such high resolution, the transitions with close excitation energies can be resolved. A typical IXS spectrum of argon is shown in Fig. 1 along with the assigned excited states. The incident photon beam is linearly polarized and its direction is in the

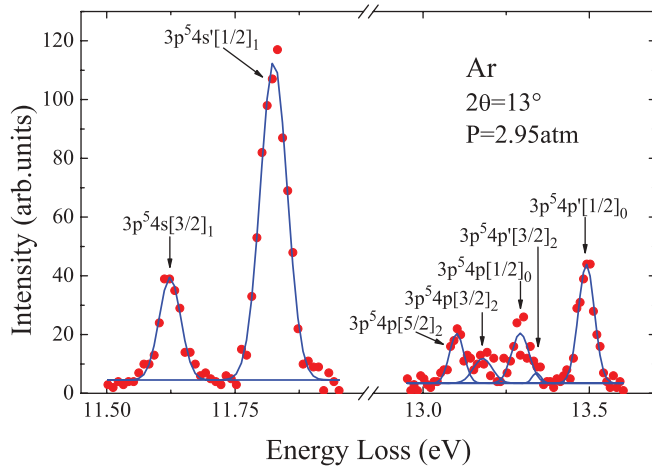


FIG. 1. (Color online) A typical inelastic x-ray scattering spectrum of argon gas. Solid red circles: experimental data; blue line: fitted results.

scattering plane. All spectra in 5° – 55° were recorded at room temperature.

The DCS for a definite excitation n in IXS can be determined by

$$\frac{d\sigma(\omega_n, 2\theta)}{d\Omega} = \frac{N(\omega_n, 2\theta)}{N_0} \frac{1}{D_0 \alpha} \frac{1}{l_{\text{eff}}} \frac{1}{n_0 P}. \quad (3)$$

Here $N(\omega_n, 2\theta)$ and N_0 stand for the counts of the transition's peak and incident photon, and the former is obtained by fitting the raw experimental spectrum while the latter is recorded by an ionization chamber in front of the gas cell [2,4]. l_{eff} , n_0 , and P are the collision length, density of the target in 1 atm, and pressure of the target in units of atm, respectively. l_{eff} is variable and it is proportional to $1/\sin 2\theta$ when the scattering angle is larger than 16° . However, the collision length l_{eff} deviates $1/\sin 2\theta$ in small scattering angles caused by the finite size of the gas cell. α is the actual transmission rate and D_0 is a factor determined by the detection efficiencies of the ionization chamber and the detector of the scattered photon. Herein D_0 is a constant because the measured energy loss region is much smaller compared with the incident photon energy, while α is determined by the sample's species and pressure in the gas cell. $\zeta(\mathbf{q}, \omega_n)$ for the $1s^2 \rightarrow 1s2p$ transition of helium [2,30–32], which has been measured and calculated with a high accuracy and proven to be reliable, was measured in small scattering angles and used to calibrate l_{eff} and normalize the results of argon. Either helium or argon was sealed in gas cell with helium at 8 atm and argon at 2.95 atm, and the smaller pressure of argon is used to reduce the absorption of photons. The actual transmission rates of argon and helium were measured to normalize the experimental data in the same experimental conditions. Noticing that the scattered photon's energy is fixed at 9888.8 eV, it is obtained from formulas (2) and (3) in small angles that

$$\zeta^{\text{Ar}}(\mathbf{q}, \omega_n) = \frac{[N(\omega_n, 2\theta)/N_0]^{\text{Ar}}}{[N(\omega_n, 2\theta)/N_0]^{\text{He}}} \frac{P^{\text{He}}}{P^{\text{Ar}}} \frac{\alpha^{\text{He}}}{\alpha^{\text{Ar}}} \frac{\omega_i^{\text{Ar}}}{\omega_i^{\text{He}}} \zeta^{\text{He}}(\mathbf{q}, \omega_n). \quad (4)$$

In $2\theta > 16^\circ$, an angular factor $\cos^2 2\theta / \sin 2\theta$ should be used to calibrate l_{eff} and $|\boldsymbol{\varepsilon}_i \cdot \boldsymbol{\varepsilon}_f^*|^2$, and only the IXS spectra of argon were measured in this angular region. Then the $\zeta(\mathbf{q}, \omega_n)$ for the valence-shell excitations of argon were determined, which will be discussed in Sec. III.

The experimental errors of $\zeta(\mathbf{q}, \omega_n)$ are attributed to the statistics of counts, the normalizing procedure, as well as the procedure of least-squares fitting; they are shown in the corresponding figures.

III. RESULTS AND DISCUSSION

Figure 1 shows that the electric monopolar excitations to $3p^5 4p[1/2]_0$ and $3p^5 4p'[1/2]_0$, the electric dipolar excitations to $3p^5 4s[3/2]_1$ and $3p^5 4s'[1/2]_1$, as well as the electric quadrupolar excitations to $3p^5 4p[5/2]_2$, $3p^5 4p[3/2]_2$, and $3p^5 4p'[3/2]_2$ are observed and resolved at the present energy resolution of about 70 meV. The squared form factors of these transitions are shown in Figs. 2, 3, and 4 and listed in Table I. The recent state-resolved results measured by high-energy EELS [7,8] and some theoretical calculations such as FBA [12] and RPAE [10,33] are also shown in Figs. 2, 3, and 4 for comparison. Since the EELS results of

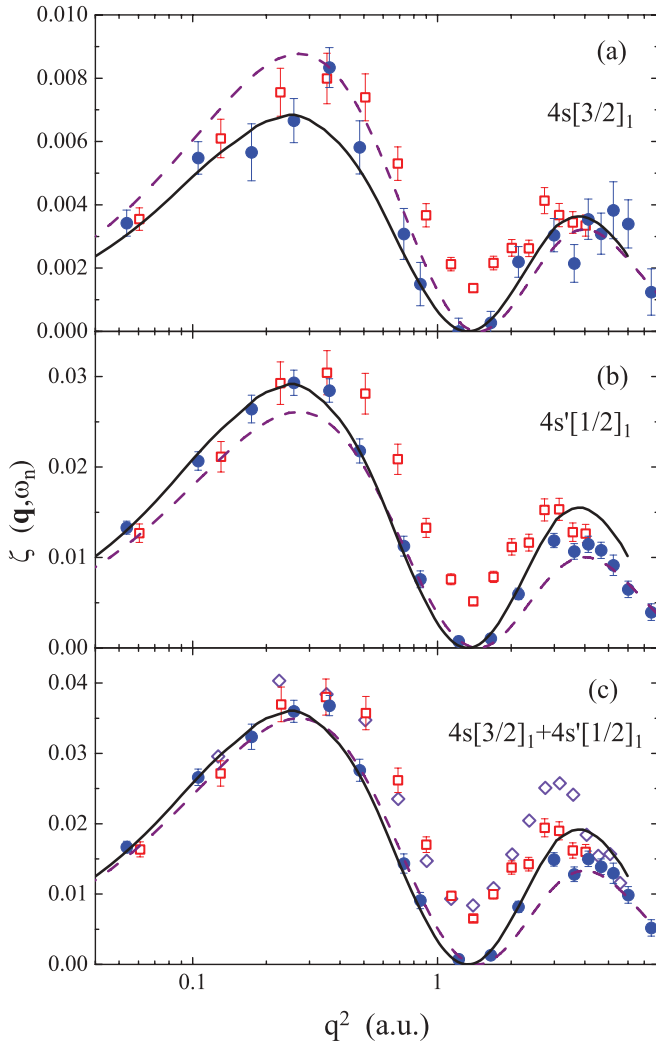


FIG. 2. (Color online) The squared form factors $\zeta(\mathbf{q}, \omega_n)$ for the electric dipolar excitations to (a) $3p^54s[3/2]_1$, (b) $3p^54s'[1/2]_1$, and (c) $3p^54s[3/2]_1 + 3p^54s'[1/2]_1$ of argon. Solid blue circles: the present IXS results; hollow red squares: the 2500 eV EELS results by Zhu *et al.* [8]; hollow violet diamonds: the 2500 eV EELS results by Fan *et al.* [7]; solid black line: RPAE calculations by Amusia *et al.* [10]; dashed purple line: FBA calculations by Vos *et al.* [12].

the dipole-forbidden transitions of Fan *et al.* [7] may include some contributions from higher neighbor transitions due to their limited energy resolution of 0.8 eV, their results were not shown in the corresponding figures except for one of the dipole-allowed transitions of $3p^54s$, which is resolved clearly in their work. Amusia *et al.* calculated the total squared form factors of the excitations with the same multiplicity in RPAE, so the intermediate coupling coefficients [8] were used to obtain separate SFF's by multiplying the RPAE results by the square of the intermediate coupling coefficients of the singlet component [8]. The results of $3p^54s[3/2]_1 + 3p^54s'[1/2]_1$ for extremely high energy EELS by Wong *et al.* [22] are not shown in the corresponding figure because they do not match those results shown in Fig. 2 in both the shape of the curve and the positions of the extrema, though the FBA should be valid for an incident electron energy of 25 keV. It is clear from Figs. 2, 3, and 4 that the SFF's for excitations with

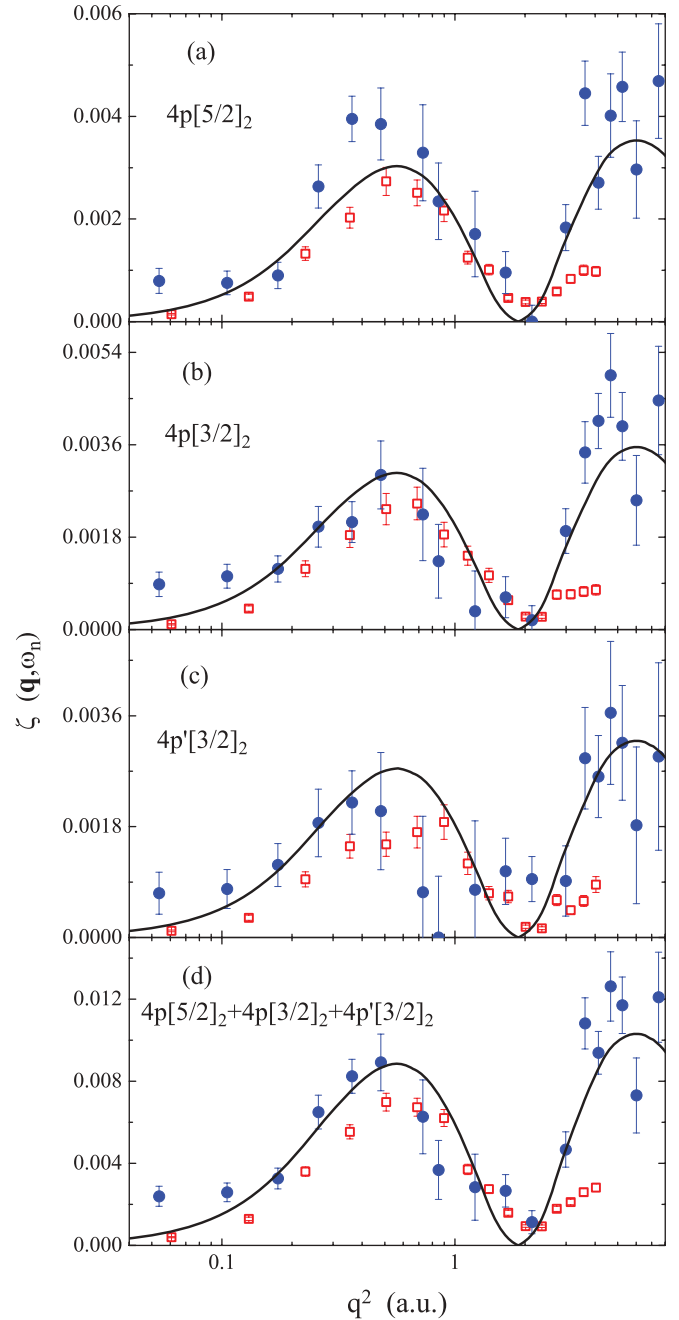


FIG. 3. (Color online) The squared form factors $\zeta(\mathbf{q}, \omega_n)$ for the electric quadrupolar excitations to (a) $3p^54p[5/2]_2$, (b) $3p^54p[3/2]_2$, (c) $3p^54p'[3/2]_2$, and (d) $3p^54p[5/2]_2 + 3p^54p[3/2]_2 + 3p^54p'[3/2]_2$ of argon. Solid blue circles: the present IXS results; hollow red squares: the 2500 eV EELS results by Zhu *et al.* [8]; solid black line: the recent RPAE calculations by Amusia *et al.* [33].

the same multiplicity have the same properties, such as the same positions of minima and maxima. We will discuss these transitions in three groups according to their multiplicity.

Figures 2(a) and 2(b) show the $\zeta(\mathbf{q}, \omega_n)$ of the electric dipolar transitions of $3p^54s[3/2]_1$ and $3p^54s'[1/2]_1$, respectively. In the investigated momentum transfer region ($q^2 < 8$ a.u.), the $\zeta(\mathbf{q}, \omega_n)$ of these electric dipolar transitions have similar shapes and the same extreme positions, i.e., two maxima and one minimum are located at about $q^2 = 0.25$ a.u., 3.6 a.u.,

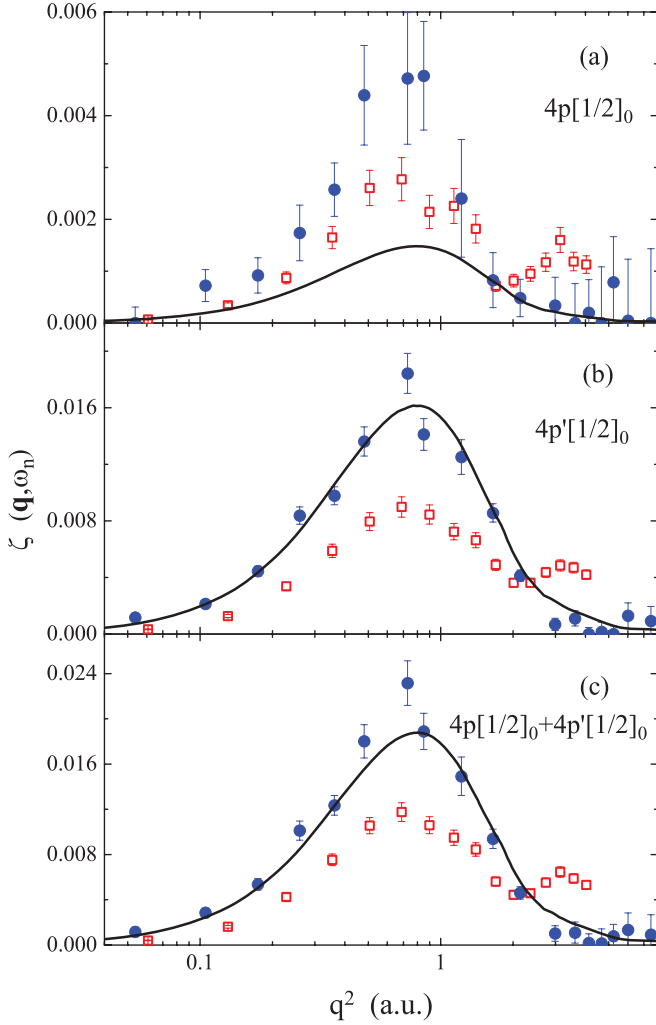


FIG. 4. (Color online) The squared form factors $\zeta(\mathbf{q}, \omega_n)$ for the electric monopolar excitations to (a) $3p^54p[1/2]_0$, (b) $3p^54p'[1/2]_0$, and $3p^54p[1/2]_0 + 3p^54p'[1/2]_0$ of argon. Solid blue circles: the present IXS results; hollow red squares: the 2500 eV EELS results by Zhu *et al.* [8]; solid black line: the recent RPAE calculations by Amusia *et al.* [33].

and 1.3 a.u., respectively. It can be seen clearly that the extreme positions calculated by RPAE [10] and FBA [12] are in excellent agreement with the experimental observations. In addition, the $\zeta(\mathbf{q}, \omega_n)$ calculated by RPAE match the present IXS results perfectly within the experimental errors except that for $3p^54s'[1/2]_1$ the RPAE calculations are somewhat larger than the IXS ones in $q^2 > 3$ a.u. However, the FBA calculations show a different result. They are in good agreement with the present IXS results in $q^2 > 1$ a.u. for $3p^54s[3/2]_1$, and in 0.5 a.u. $< q^2 < 1.5$ a.u. and $q^2 > 3.5$ a.u. for $3p^54s'[1/2]_1$, while they apparently deviate from the IXS results in other q^2 regions, i.e., they somewhat overestimate the IXS $\zeta(\mathbf{q}, \omega_n)$ of $3p^54s[3/2]_1$ in $q^2 < 1$ a.u. and underestimate the IXS $\zeta(\mathbf{q}, \omega_n)$ of $3p^54s'[1/2]_1$ in $q^2 < 0.5$ a.u. and 1.5 a.u. $< q^2 < 3.5$ a.u.. The sum of the $\zeta(\mathbf{q}, \omega_n)$ of $3p^54s[3/2]_1$ and $3p^54s'[1/2]_1$ is presented in Fig. 2(c). An excellent consistency between the IXS results and two theoretical calculations is observed in $q^2 < 1.5$ a.u., so there is some evidence to say that interactions, including the exchange effect, are not remarkable for the

electric dipolar transitions of $3p^54s$ in this q^2 region. However, it seems that the RPAE calculations match the IXS results slightly better than the FBA results in 1.5 a.u. $< q^2 < 3$ a.u., while the situation is reversed in $q^2 > 3$ a.u.. In our previous investigations of He [2,4] and Ne [5], the FBA or RPAE calculations match the IXS results excellently in the whole measured q^2 region, but the aforementioned phenomenon of argon is different. The reason may be that argon is heavier than helium and neon, and it is more difficult to acquire its accurate wave functions and to deal with the electronic correlations. Therefore, more theoretical works are recommended to clarify this phenomenon.

It can be seen from Fig. 2 that the $\zeta(\mathbf{q}, \omega_n)$ measured by the high-energy EELS at 2500 eV are in good agreement with the present IXS results in $q^2 < 0.4$ a.u. and $q^2 > 4$ a.u., while the former are much larger than the latter in 0.4 a.u. $< q^2 < 4$ a.u. It should be stressed that the EELS results measured at 2500 eV by different groups [7,8] with different normalization methods and different energy resolutions are in good agreement except for four points as shown in Fig. 2(c); this demonstrates the reliability of two sets of the EELS data. The enhanced part of the EELS results in 0.4 a.u. $< q^2 < 4$ a.u. should be due to intramolecular multiple scattering [3,5], which comes from the contributions of the second Born scattering amplitude and may be explained by the calculation of the second Born approximation (SBA). However, the SBA calculation has been absent until now, to the best of our knowledge. Similar behaviors have been observed for neon [5] and nitrogen [3], and it seems that the intramolecular multiple scattering is more severe for neon than for argon, which is somewhat strange because intramolecular multiple scattering should be more important for heavier atoms, as pointed out by Bradley *et al.* [3]. The reason for this is unclear, and more theoretical and experimental works are required to elucidate it.

The $\zeta(\mathbf{q}, \omega_n)$ of the electric quadrupolar transitions of $3p^54p[5/2]_2$, $3p^54p[3/2]_2$, and $3p^54p'[3/2]_2$ are shown in Figs. 3(a), 3(b), and 3(c), respectively, and their sum is shown in Fig. 3(d). Compared with the $\zeta(\mathbf{q}, \omega_n)$ of the electric dipolar transitions of $3p^54s[3/2]_1$ and $3p^54s'[1/2]_1$, the $\zeta(\mathbf{q}, \omega_n)$ of the electric quadrupolar transitions of $3p^54p[5/2]_2$, $3p^54p[3/2]_2$, and $3p^54p'[3/2]_2$ have larger experimental errors because of their low intensities and narrow energy intervals as shown in Fig. 1, especially for $3p^54p'[3/2]_2$ since it overlaps with $3p^54p[1/2]_0$. Like the $\zeta(\mathbf{q}, \omega_n)$ of the electric dipolar excitations, the $\zeta(\mathbf{q}, \omega_n)$ of the electric quadrupolar excitations have two maxima and one minimum in $q^2 < 8$ a.u., although it is difficult to determine the position of the second maximum. In detail, the first maximum is at about 0.5 a.u. and the minimum is at about 2 a.u. It is noticed that the second maximum is larger than the first maximum for the electric quadrupolar excitations, while the situation is reversed for the electric dipolar excitations. This indicates that in the large q^2 region, the electric quadrupolar excitations dominate.

Considering the larger experimental errors of the electric quadrupolar transitions as mentioned above, the present IXS results shown in Fig. 3 are in good agreement with the RPAE calculations and in reasonable agreement with the previous EELS ones at 2500 eV in $q^2 < 2$ a.u., although the present

TABLE I. Squared formed factors of valence-shell excitations of argon.

q^2	$3p^54s[3/2]_1$	$3p^54s'[1/2]_1$	$3p^54p[5/2]_2$	$3p^54p[3/2]_2$	$3p^54p[1/2]_0$	$3p^54p'[3/2]_2$	$3p^54p'[1/2]_0$
0.053	3.4[-3]	1.3[-2]	7.9[-4]	8.8[-4]	4.7[-10]	7.2[-4]	1.2[-3]
0.105	5.5[-3]	2.1[-2]	7.6[-4]	1.0[-3]	7.2[-4]	7.9[-4]	2.1[-3]
0.174	5.7[-3]	2.6[-2]	9.0[-4]	1.2[-3]	9.2[-4]	1.2[-3]	4.5[-3]
0.259	6.7[-3]	2.9[-2]	2.6[-3]	2.0[-3]	1.7[-3]	1.9[-3]	8.4[-3]
0.361	8.3[-3]	2.8[-2]	4.0[-3]	2.1[-3]	2.6[-3]	2.2[-3]	9.8[-3]
0.480	5.8[-3]	2.2[-2]	3.9[-3]	3.0[-3]	4.4[-3]	2.1[-3]	1.4[-2]
0.729	3.1[-3]	1.1[-2]	3.3[-3]	2.2[-3]	4.7[-3]	7.4[-4]	1.8[-2]
0.850	1.5[-3]	7.6[-3]	2.4[-3]	1.3[-3]	4.8[-3]	7.1[-9]	1.4[-2]
1.22	3.3[-9]	7.3[-4]	1.7[-3]	3.6[-4]	2.4[-3]	7.7[-4]	1.3[-2]
1.65	2.7[-4]	1.1[-3]	9.6[-4]	6.3[-4]	8.3[-4]	1.1[-3]	8.6[-3]
2.14	2.2[-3]	6.0[-3]	4.7[-9]	1.8[-4]	4.8[-4]	9.5[-4]	4.1[-3]
2.99	3.0[-3]	1.2[-2]	1.8[-3]	1.9[-3]	3.4[-4]	9.2[-4]	6.8[-4]
3.62	2.2[-3]	1.1[-2]	4.5[-3]	3.5[-3]	8.9[-10]	2.9[-3]	1.1[-3]
4.13	3.5[-3]	1.1[-2]	2.7[-3]	4.1[-3]	2.0[-4]	2.6[-3]	2.0[-9]
4.67	3.1[-3]	1.1[-2]	4.0[-3]	5.0[-3]	1.5[-8]	3.7[-3]	1.5[-4]
5.23	3.8[-3]	9.1[-3]	4.6[-3]	4.0[-3]	7.9[-4]	3.2[-3]	2.7[-9]
6.01	3.4[-3]	6.5[-3]	3.0[-3]	2.5[-3]	4.7[-5]	1.8[-3]	1.3[-3]
7.48	1.2[-3]	4.0[-3]	4.7[-3]	4.5[-3]	5.6[-10]	2.9[-3]	9.2[-4]

results are generally larger than the EELS ones. However, the present IXS $\zeta(\mathbf{q}, \omega_n)$ in $q^2 > 2$ a.u. are much larger than the EELS ones at 2500 eV, which indicates that the FBA has not been reached in $q^2 > 2$ a.u., even at an impact energy of 2500 eV. In our previous investigations of neon, the EELS results for the electric quadrupolar excitations at 2500 eV were in reasonable agreement with the IXS ones and RPAE calculations in the whole q^2 region of $q^2 < 6$ a.u. The reason for the disagreement in $q^2 > 2$ a.u. of argon may be that argon has a larger atomic number, and it is more difficult to satisfy the FBA.

Figure 4 shows the $\zeta(\mathbf{q}, \omega_n)$ of the electric monopolar excitations to $3p^54p[1/2]_0$, $3p^54p'[1/2]_0$, and their sum. Unlike the $\zeta(\mathbf{q}, \omega_n)$ of the electric dipolar and quadrupolar excitations, the electric monopolar excitations have only one maximum at about $q^2 = 0.7$ a.u. and no minimum. It is clear in Fig. 4(a) that the $\zeta(\mathbf{q}, \omega_n)$ of IXS for $3p^54p[1/2]_0$ is much larger than that of RPAE at $q^2 < 1.5$ a.u., while they are in good agreement at $q^2 > 1.5$ a.u.. Despite this difference, the $\zeta(\mathbf{q}, \omega_n)$ of the IXS and RPAE for $3p^54p'[1/2]_0$ show excellent consistency, as shown in Fig. 4(b). Since the intensities of $3p^54p[1/2]_0$ are relatively small, i.e., they are about 25% of those of $3p^54p'[1/2]_0$, the $\zeta(\mathbf{q}, \omega_n)$ of $3p^54p[1/2]_0 + 3p^54p'[1/2]_0$ are in good agreement with the RPAE calculations in the whole q^2 region. However, the higher values of $3p^54p[1/2]_0$ result in the IXS ones of $3p^54p[1/2]_0 + 3p^54p'[1/2]_0$ being slightly larger than the RPAE results in $q^2 < 0.65$ a.u., as shown in Fig. 4(c).

In $q^2 < 2$ a.u., the apparent squared form factor $\zeta^A(\mathbf{q}, \omega_n)$ [4] of the EELS at 2500 eV are much smaller than the present $\zeta(\mathbf{q}, \omega_n)$ of IXS, while the situation is reversed in $q^2 > 2$ a.u., as shown in Figs. 4(a), 4(b), and 4(c). In addition, the $\zeta^A(\mathbf{q}, \omega_n)$ of EELS have a second maximum at about 3 a.u. and form a shoulder which is absent in the IXS results and RPAE calculations. Similar character can be noticed for the electric monopolar excitations of neon [5], although the shoulder at $q^2 = 3$ a.u. in EELS results at 2500 eV is not very clear while

the second maximum is very strong in EELS ones measured at moderate impact energies of 300–500 eV [34]. The large difference between the present IXS $\zeta(\mathbf{q}, \omega_n)$ and the previous EELS $\zeta^A(\mathbf{q}, \omega_n)$ at 2500 eV means that the FBA is not satisfied for the electric monopolar transitions, even at a high impact energy of 2500 eV. Such phenomena can be understood, as it is well known that the higher-order Born amplitudes provide the main contribution to the apparent $\zeta^A(\mathbf{q}, \omega_n)$ for transitions in which the terms of the initial and final states are the same, as in the case of $^1S_0 \rightarrow ^1S_0$ transition, as pointed out by Suzuki *et al.* [9].

IV. SUMMARY AND CONCLUSION

Using high-resolution IXS, the state-resolved squared form factors $\zeta(\mathbf{q}, \omega_n)$ of the electric monopolar excitations to $3p^54p[1/2]_0$ and $3p^54p'[1/2]_0$, the electric dipolar excitations to $3p^54s[3/2]_1$ and $3p^54s'[1/2]_1$, and the electric quadrupolar excitations to $3p^54p[5/2]_2$, $3p^54p[3/2]_2$, and $3p^54p'[3/2]_2$ of argon are determined at an incident photon energy of about 10 keV and target pressure of 2.95 atm. The present IXS results give the benchmark data of valence-shell excitations of argon. Different from previous IXS investigations of neon in which the IXS results are in excellent agreement with the RPAE calculations in the whole measured q^2 region, the present IXS results show obvious differences from the RPAE calculations in $q^2 > 3$ a.u. for the electric dipolar excitation of $3p^54s'[1/2]_1$, and in $q^2 < 1.5$ a.u. for the electric monopolar excitation of $3p^54p[1/2]_0$, although the present IXS results for these two excitations in other q^2 regions and for other excitations in the whole measured q^2 region are in good agreement with the RPAE results. This phenomenon means that for the heavier atom of argon it is more difficult to obtain its accurate wave functions or to deal with the electronic correlations. By comparing the present IXS results with the high-energy EELS ones, it is found that for the valence-shell excitations of argon the FBA may not even be reached at an

incident electron energy of 2.5 keV in the electron scattering process. Further state-resolved experimental and theoretical investigations are highly recommended.

ACKNOWLEDGMENTS

This work is supported by the National Natural Science Foundation of China (Grants No. 10979040 and No.

11104309), the National Basic Research Program of China (Grant No. 2010CB923301), the Research Fund for the Doctoral Program of Higher Education of China, and the Fundamental Research Funds for Central Universities. The experiment was carried out in a beamtime approved by Japan Synchrotron Radiation Research Institute (Proposal No. 2011B4256) and the National Synchrotron Radiation Research Center, Taiwan, Republic of China (No. 2010-3-073-4).

-
- [1] U. Fano and A. R. P. Rau, *Atomic Collisions and Spectra* (Academic, Orlando, FL, 1986).
- [2] B. P. Xie, L. F. Zhu, K. Yang, B. Zhou, N. Hiraoka, Y. Q. Cai, Y. Yao, C. Q. Wu, E. L. Wang, and D. L. Feng, *Phys. Rev. A* **82**, 032501 (2010).
- [3] J. A. Bradley, G. T. Seidler, G. Cooper, M. Vos, A. P. Hitchcock, A. P. Sorini, C. Schlimmer, and K. P. Nagle, *Phys. Rev. Lett.* **105**, 053202 (2010).
- [4] L. F. Zhu, L. S. Wang, B. P. Xie, K. Yang, N. Hiraoka, Y. Q. Cai, and D. L. Feng, *J. Phys. B: At. Mol. Opt. Phys.* **44**, 025203 (2011).
- [5] L. F. Zhu, W. Q. Xu, K. Yang, Z. Jiang, X. Kang, B. P. Xie, D. L. Feng, N. Hiraoka, and K. D. Tsuei, *Phys. Rev. A* **85**, 030501(R) (2012).
- [6] G. P. Li, T. Takayanagi, K. Wakiya, H. Suzuki, T. Ajiro, S. Yagi, S. S. Kano, and H. Takuma, *Phys. Rev. A* **38**, 1240 (1988).
- [7] X. W. Fan and K. T. Leung, *Phys. Rev. A* **62**, 062703 (2000).
- [8] L. F. Zhu, H. D. Cheng, Z. S. Yuan, X. J. Liu, J. M. Sun, and K. Z. Xu, *Phys. Rev. A* **73**, 042703 (2006).
- [9] T. Y. Suzuki, H. Suzuki, S. Ohtani, T. Takayanagi, and K. Okada, *Phys. Rev. A* **75**, 032705 (2007).
- [10] Z. Chen, A. Z. Msezane, and M. Y. Amusia, *Phys. Rev. A* **60**, 5115 (1999).
- [11] M. Y. Amusia, L. V. Chernysheva, Z. Felfli, and A. Z. Msezane, *Phys. Rev. A* **65**, 062705 (2002).
- [12] M. Vos, R. P. McEachran, G. Cooper, and A. P. Hitchcock, *Phys. Rev. A* **83**, 022707 (2011).
- [13] A. N. Hopersky, A. M. Nadolinsky, K. K. Ikoeva, and O. A. Khoroshavina, *J. Exp. Theor. Phys.* **113**, 731 (2011).
- [14] A. N. Hopersky, A. M. Nadolinsky, K. K. Ikoeva, and O. A. Khoroshavina, *J. Phys. B: At. Mol. Opt. Phys.* **44**, 145202 (2011).
- [15] J. Lehtola, M. Hakala, J. Vaara, and K. Hamalainen, *Phys. Chem. Chem. Phys.* **13**, 5630 (2011).
- [16] J. A. Bradley, A. Sakko, G. T. Seidler, A. Rubio, M. Hakala, K. Hamalainen, G. Cooper, A. P. Hitchcock, K. Schlimmer, and K. P. Nagle, *Phys. Rev. A* **84**, 022510 (2011).
- [17] A. Sakko, S. Galambosi, J. Inkinen, T. Pylkkanen, M. Hakala, S. Huotari, and K. Hamalainen, *Phys. Chem. Chem. Phys.* **13**, 11678 (2011).
- [18] M. A. Khakoo, P. Vandeventer, J. G. Childers, I. Kanik, C. J. Fontes, K. Bartschat, V. Zeman, D. H. Madison, S. Saxena, R. Srivastava *et al.*, *J. Phys. B: At. Mol. Opt. Phys.* **37**, 247 (2004).
- [19] M. Allan, O. Zatsarinny, and K. Bartschat, *Phys. Rev. A* **74**, 030701 (2006).
- [20] S. Mondal, J. Lower, S. J. Buckman, R. P. McEachran, G. Garcia, O. Zatsarinny, and K. Bartschat, *PMC Phys. B* **2**, 3 (2009).
- [21] M. A. Khakoo, O. Zatsarinny, and K. Bartschat, *J. Phys. B: At. Mol. Opt. Phys.* **44**, 015201 (2011) and the references therein.
- [22] T. C. Wong, J. S. Lee, and R. A. Bonham, *Phys. Rev. A* **11**, 1963 (1975).
- [23] C. E. Bielschowsky, G. G. B. de Souza, C. A. Lucas, and H. M. Boechat Roberty, *Phys. Rev. A* **38**, 3405 (1988).
- [24] Q. Ji, S. L. Wu, R. F. Feng, X. J. Zhang, L. F. Zhu, Z. P. Zhong, K. Z. Xu, and Y. Zheng, *Phys. Rev. A* **54**, 2786 (1996).
- [25] L. F. Zhu, H. Yuan, W. C. Jiang, F. X. Zhang, Z. S. Yuan, H. D. Cheng, and K. Z. Xu, *Phys. Rev. A* **75**, 032701 (2007).
- [26] R. A. Bonham, *J. Chem. Phys.* **36**, 3260 (1962).
- [27] I. Shimamura, *J. Phys. Soc. Jpn.* **30**, 824 (1971).
- [28] P. M. Platzman and N. Tzoar, *Phys. Rev.* **139**, A410 (1965).
- [29] P. Eisenberger and P. M. Platzman, *Phys. Rev. A* **2**, 415 (1970).
- [30] N. M. Cann and A. J. Thakkar, *J. Electron Spectrosc. Relat. Phenom.* **123**, 143 (2002).
- [31] X. J. Liu, L. F. Zhu, Z. S. Yuan, W. B. Li, H. D. Cheng, J. M. Sun, and K. Z. Xu, *J. Electron Spectrosc. Relat. Phenom.* **135**, 15 (2004).
- [32] X. Y. Han and J. M. Li, *Phys. Rev. A* **74**, 062711 (2006).
- [33] M. Y. Amusia, L. V. Chernysheva, and V. G. Yarzhevsky, *Atomic Data: Photon Absorption, Electron Scattering, Vacancy Decay* (Nauka, Saint Petersburg, 2010) [in Russian].
- [34] T. Y. Suzuki, H. Suzuki, S. Ohtani, B. S. Min, T. Takayanagi, and K. Wakiya, *Phys. Rev. A* **49**, 4578 (1994).